

Time-dependent Real-space Renormalization-Group Approach: application to an adiabatic random quantum Ising model

Peter Mason, Alexandre M. Zagoskin and Joseph J. Betouras

Department of Physics, Loughborough University, Loughborough, LE11 3TU, United Kingdom

Abstract. We develop a time-dependent real-space renormalization-group approach which can be applied to Hamiltonians with time-dependent random terms. To illustrate the renormalization-group analysis, we focus on the quantum Ising Hamiltonian with random site- and time-dependent (adiabatic) transverse-field and nearest-neighbour exchange couplings. We demonstrate how the method works in detail, by calculating the off-critical flows and recovering the ground state properties of the Hamiltonian such as magnetization and correlation functions. The quantum critical point, or points, depend on time through the time-dependence of the parameters of the Hamiltonian. We, furthermore, make connections with Kibble-Zurek dynamics and provide a scaling argument for the density of defects as we adiabatically pass through the critical point of the system.

I. Introduction

An interacting quantum system evolving at zero temperature can demonstrate various forms of approach to equilibrium even with no loss of phase coherence. In the past, detailed experimental [1] and theoretical studies [2, 3, 4, 5, 6, 7] for systems prepared by a quantum quench across a phase transition have studied this kind of out-of-equilibrium path. A system is prepared in the ground state for certain values of parameters, which are then rapidly changed to values for which the ground state (GS) is known to be in a different phase. Experiments on ultracold atoms are particularly useful to probe this physics because they are essentially closed quantum systems on rather long time scales compared to the basic dynamical time scales of the system. As such, fundamental questions as to whether many physical properties equilibrate after the quench exponentially in time and the system thermalizes (so it can be described by an effective temperature) can be addressed.

Apart from instant quenches of an interacting quantum system, there is much attention on those Hamiltonians which change smoothly across a quantum phase transition [8, 9, 10, 11, 12]. In general a single tunable parameter, or perturbation, is chosen to address this transition, and the non-equilibrium dynamics such as the growth of density defects or entanglement entropy is then studied as a function of this parameter. For a second-order transition critical point, various averaged physical quantities such as the excitation density and energy show power laws as the rate of change approaches zero, with exponents determined by the universal physics of the quantum critical point. The system evolves after such a sweep to a steady state for some quantities, but its energy distribution remains nonthermal [11].

Quantum spin chains provide prime examples of the interacting quantum systems where the evolution of out-of-equilibrium many-body systems [13], that possess many degrees of freedom, is theoretically illustrated. The addition of disorder in the system provides another dimension which needs to be addressed. The properties of quantum spin chains with quenched randomness at low temperatures have been the subject of interest for a number of years. In the case of a one-dimensional transverse-field quantum Ising model with randomness, a renormalization-group (RG) treatment shows that the disorder grows without bound [15, 16, 14] - the flow is towards an infinite-randomness fixed point. This strong disorder renormalization-group approach has seen further successful progress and development to tackle issues related to many-body localisation in interacting models with disorder [17, 18], such as establishing the form of the growth of the entropy in an XXZ spin-chain [20, 19], as well as establishing the physics around the phase transition between the many-body localised phase and the thermal phase for a general interacting model [21, 22, 23, 24, 25], and investigating Floquet dynamics in periodically driven random quantum spin chains [26, 27].

In the present work, we address the problem of a random quantum spin chain, requiring control of more than one parameter as we pass through a quantum critical point. We will as such concentrate on an adiabatic quantum Hamiltonian. This is

also an important question in the field of adiabatic quantum computation, with a time-dependent Hamiltonian of the generic form

$$H(t) = H_{\text{initial}}(t) + H_{\text{final}}(t), \quad (1)$$

subject to initial conditions that $H_{\text{final}}(0) = 0$ and final conditions that $H_{\text{initial}}(T) = 0$, where T is the end-point of the computation. The ground, and easily reachable, state of the initial Hamiltonian, H_{initial} , is assumed known, whereas the ground state of the final Hamiltonian at $t = T$, H_{final} , is unknown and encodes the desired solution to the computation. The adiabatic evolution of the Hamiltonian is such that the computation always remains in, or close to, the local ground state at some given instant in time. Crucially, the computation will therefore terminate in the ground state of H_{final} .

The inclusion of adiabatic parameters means that the energy gap between the ground state and first excited state is now necessarily time-dependent, such that it can increase or decrease depending on the rate of the computation. As such, remaining in the ground state, or removing any excited states, requires the adiabatic process to progress sufficiently slowly. However, if the quantum Hamiltonian exhibits a quantum critical point, the energy gap will, at this point, decrease to zero, and the computation will lose adiabaticity. For the quantum computation therefore, the transition through the quantum critical point will lead to the development of excited states, or defects, the density of which depend on the rate of transition.

We address the issue of a generic time dependence in the quantum Hamiltonian (Eq. (1)), focussing on developing a complete analysis of both the ground states as well as the dynamics across a quantum critical point. The time-dependence (as we will see) provides a tool to shift in time the location of the quantum critical point. This is particularly important in the development of a device to simulate the quantum critical point. Optimisation problems commonly in the NP-complete and NP-hard classes can be mapped onto an Ising model [28, 29] (indeed the architecture of, for example the D:Wave machines [30, 31], is designed to use a quantum adiabatic protocol, and run based on an adiabatic quantum Ising Hamiltonian). As such we will concentrate our analysis on an adiabatic Ising Hamiltonian with random transverse-fields and exchange couplings, but simplify the setup to consider an infinitely long one-dimensional chain of Ising spins. Such 1D spin chains governed by a quantum Ising Hamiltonian can be experimentally realised as flux qubits; see for instance [33, 32].

The strong-disorder RG approach that we develop is the time-dependent extension of that formulated in detail for the time-independent transverse-field Ising Hamiltonian by D. S. Fisher in a series of papers in the 1990's [15, 16, 14]. The work was based on the perturbative technique developed by Dasgupta and Ma [34] that safely allows for the systematic removal of the high-energy degrees of freedom on the spin-1/2 Heisenberg chain. The approach that we will employ, renormalising the bond and exchange couplings at any given instant in time, will provide access to the (local in time) properties, such as the magnetisation or correlation lengths, of the ground state, be that in the paramagnetic state or the ferromagnetic state. We will also be able to

analyse the off-critical flows around the single quantum critical point and to establish the conditions for a time-dependent duality across this critical point. This analysis of the ground state properties enables us to investigate the non-equilibrium dynamics which follows the Kibble-Zurek mechanism [8, 9, 10, 35, 36, 37] as the governing Hamiltonian (Eq. (1)) is transitioned adiabatically through the critical point. We are then able to provide a characteristic rate of adiabatic transition across the critical point and link this rate to a cut-off energy scale related to the validity of the RG scheme.

The paper is organised as follows: in Sect. II we outline the main steps in the renormalization-group approach, focussing on the one-dimensional random transverse-field Ising model and the (adiabatic) time conditions under which this approach is valid. We are able to establish the forms of the distribution functions for the transverse-field and exchange couplings as functions of the lengthscale trajectories. These allow us to identify a measure of the distance - as a function of time - from the quantum critical point separating the paramagnetic ground state from the ferromagnetic ground state. Section III identifies a critical time scale based on the adiabatic coupling parameters and uses a scaling argument to provide an estimate for the density of defects as we transition through the quantum critical point. We conclude with a discussion in Sect. IV.

II. The Real-Space Renormalization-Group Approach

In this section we present the analysis of the adiabatic Ising Hamiltonian in the strong disorder limit. We concentrate on a renormalization-group (RG) approach and discuss the role that time plays as well as the underlying conditions of the analysis. Then, we proceed by writing down the coupled integro-differential RG flow equations that govern the distribution of the random variables in our model.

A. The Adiabatic Random Quantum Ising Hamiltonian

To illustrate the approach, we study the nearest neighbour time-dependent random transverse-field Ising Hamiltonian

$$H(t) = - \sum_{i=1}^N h_i(t) \sigma_i^x - \sum_{\langle i,j \rangle}^N J_{ij}(t) \sigma_i^z \sigma_j^z \quad (2)$$

on the one-dimensional infinite chain, where the parameters $h_i(t)$ and $J_{ij}(t)$ are time-dependent random variables and denote the transverse fields and the nearest-neighbour interactions, respectively. To study the adiabatic evolution of the fixed point distributions of the above Hamiltonian the following boundary conditions are imposed:

$$J_{ij}(0) = 0, \quad h_i(T) = 0, \quad (3)$$

so that the evolution runs for times $t \in [0, T]$, with beginning- and end-point Hamiltonians given by

$$H_{\text{initial}} \equiv H(t=0) = - \sum_i^N h_i(0) \sigma_i^x, \quad (4a)$$

$$H_{\text{final}} \equiv H(t=T) = - \sum_{\langle i,j \rangle}^N J_{ij}(T) \sigma_i^z \sigma_j^z, \quad (4b)$$

respectively.

The governing Hamiltonian, Equation (2), is termed the *adiabatic* random quantum Ising model (ARQIM). This is to be contrasted to the *non-adiabatic* random quantum Ising Hamiltonian, considered by, amongst others, Fisher [14], that can be thought of as a special case of the model studied here, and occurs when $h_i(t)$ and $J_{ij}(t)$ are no longer functions of time. A further special case of the ARQIM occurs when $t = T$, at which point $B(T) = 0$, and we obtain the classical Ising model (that is identical to the end-point Hamiltonian, H_{final} , given above).

A transformation can be performed on the ARQIM by taking

$$\tau_i^z = \prod_{j \leq i} \sigma_j^x, \quad \tau_i^x = \sigma_i^z \sigma_{i+1}^z, \quad (5)$$

such that, on exchange of the $h_i(t)$ and $J_{ij}(t)$, the ARQIM is recovered again: this identifies a duality transformation $h_i(t) \longleftrightarrow J_{ij}(t)$, a feature that will be used in the RG analysis later in this section. In analogy with the non-adiabatic Hamiltonian, subject to certain conditions that we discuss below, the ARQIM contains a quantum critical point which relates the magnitudes of the site and bond couplings, $h_i(t)$ or $J_{ij}(t)$. For now, there are no restrictions on these relative magnitudes, however at a later stage, the limit around, and the dynamics across, the critical point, $\delta(t) = 0$ will be studied. This is defined as

$$\delta(t) \approx \frac{\Delta_{h(t)} - \Delta_{J(t)}}{\text{Var}(\log(J(t))) + \text{Var}(\log(h(t)))}, \quad (6)$$

where $\Delta_{h(t)} = \overline{\log(h(t))}$, $\Delta_{J(t)} = \overline{\log(J(t))}$, and where $J(t)$ and $h(t)$ are the sets that contain the $J_{ij}(t)$ and $h_i(t)$. The single critical point occurs when $\delta(t) = 0$, which occurs when $\Delta_{h(t)} = \Delta_{J(t)}$. If $\delta(t) > 0$ then the ground state under the renormalization procedure will be paramagnetic, whereas in the other limit, $\delta(t) < 0$, the ground state will be ferromagnetic. Either side of the critical point rare regions effects are important; these Griffiths phases persist well into the paramagnetic or ferromagnetic regions, however we note that our boundary conditions (Eq. (3)) impose that at some $\delta(t)$ both paramagnetic and ferromagnetic rare region effects are lost [38, 39, 40].

B. The Role of Time

At this stage it is appropriate to discuss the role of time in the renormalization procedure. It is important to note the distinction that is made between the renormalization steps

and the time evolution: the renormalization will take place *at a fixed time*. Time enters the renormalization procedure parametrically/as a trajectory through the distribution functions of the $J(t) = \{J_{ij}(t)\}$ and $h(t) = \{h_i(t)\}$, and through the length scales. As a consequence, the renormalization leads to the low-energy fixed point ground state solution, that is either paramagnetic ($\delta(t) > 0$) or ferromagnetic ($\delta(t) < 0$). Here, time play the role of a weighting on the random couplings, thus influencing the form of the ground state. As a result the magnetisation scalings and the correlation length scalings also become time dependent implicitly through a length scale trajectory and/or the criticality parameter $\delta(t)$.

After the renormalization procedure, for a given time, has completed and the ground state solution has been found, we move ($t \rightarrow t + dt$) to the next time instance and re-perform the renormalization. The process is then repeated until the desired end-time. Since we are only interested in adiabatic time flow, we expect that, for a given initial choice of $J(t)$'s and $h(t)$'s, we would not excite any states above the ground state as we time evolve, provided we are sufficiently far from the critical point, $\delta(t) = 0$. We address the question as to the density of excited states as we approach and cross the critical point in Sect. III.

By writing $h_i(t) = B_i(t)\tilde{h}_i$ and $J_{ij}(t) = A_{ij}(t)\tilde{J}_{ij}$, the time-dependence of $h_i(t)$ and $J_{ij}(t)$ can separated out. Then \tilde{h}_i and \tilde{J}_{ij} are strictly time-independent independent random distributions, and $A_{ij}(t)$ and $B_i(t)$ are (adiabatic) bond/site-dependent non-random, hence controllable, functions. The form of the time-dependent functions $A_{ij}(t)$ and $B_i(t)$ are, at this stage, left entirely general and independent, and for the majority of our analysis we will work with the functions $h_i(t)$ and $J_{ij}(t)$, i.e. we will not assume that the time dependence can be separated out from the random variables. However, in order to clarify the RG procedure or the physics, we will at various stages separate out the time dependence.

In the case that we can separate out the time-dependence, Eq. (6) can be written as

$$\delta(t) \approx \frac{\Delta_{\tilde{h}} - \Delta_{\tilde{J}} - \Delta_t}{\text{Var}(\log(\tilde{J})) + \text{Var}(\log(\tilde{h}))}, \quad (7)$$

where $\Delta_{\tilde{h}} = \overline{\log(\tilde{h})}$, $\Delta_{\tilde{J}} = \overline{\log(\tilde{J})}$ and $\Delta_t = \log(\overline{A(t)}/\overline{B(t)})$, and where \tilde{J} , \tilde{h} , $A(t)$ and $B(t)$ are the sets that contain the \tilde{J}_{ij} , \tilde{h}_i , $A_{ij}(t)$ and $B_i(t)$, respectively. In particular, Δ_t can take positive ($\overline{A(t)} > \overline{B(t)}$) or negative ($\overline{A(t)} < \overline{B(t)}$) values (note that $\Delta_t \in [-\infty, \infty]$). The inclusion of a time dependence in the Hamiltonian gives rise to the Δ_t parameter, the value of which (either positive or negative) can influence the ground state properties of the system. Schematically, the critical line as a function of $\Delta_{\tilde{h}} - \Delta_{\tilde{J}}$ and Δ_t is presented in Fig. 1.

In Fig. 2 we give two schematic viewpoints of the time-flow under the supposition that $\Delta_{\tilde{h}} = \Delta_{\tilde{J}}$ throughout. Figure 2(a) further supposes that $A(t) = A_{ij}(t)$ and $B(t) = B_i(t) \forall i, j$ (here we choose $A(t) = 1 - B(t) = (t/T)^2$, but in general they can take any form). There then exists a single quantum critical point at $t = t_f$, where $A(t) = B(t)$, such that for $\delta(t) > 0$ (equivalently $t < t_f$) the ground state

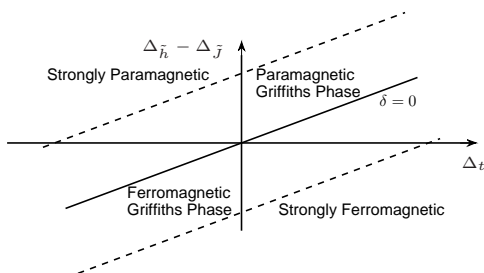


Figure 1. The critical line, $\delta(t) = 0$ separating the paramagnetic ($\delta(t) > 0$) from the ferromagnetic ($\delta(t) < 0$) region.

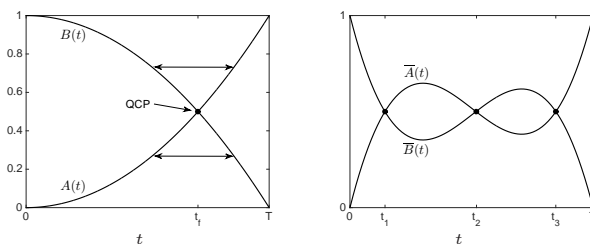


Figure 2. Schematic time-flow under the supposition that $\Delta_{\bar{h}} = \Delta_{\bar{j}}$ throughout. (a) $A(t) = A_{ij}(t)$ and $B(t) = B_i(t) \forall i, j$. There is a quantum critical point (QCP) which occurs when $t = t_f$ and $\delta(t) = 0$, here indicated at the point when $A(t_f) = B(t_f)$. The ground state is paramagnetic for $t < t_f$ and ferromagnetic for $t > t_f$. A duality in time exists across the critical point, as indicated by the double sided arrows. (b) The $A_{ij}(t)$ and $B_i(t)$ are taken to be in general distinct: shown are the mean functions $\bar{A}(t)$ and $\bar{B}(t)$. There exist multiple (here three) quantum critical points when $\Delta_t = 0$, at $t = t_1, t_2$ and t_3 .

is paramagnetic, whereas for $\delta(t) < 0$ (equivalently $t > t_f$) the ground state is ferromagnetic. In contrast Fig. 2(b) takes the $A_{ij}(t)$ and $B_i(t)$ to be in general distinct, and shows the existence of multiple quantum critical points, all located at $\Delta_t = 0$ when $\bar{A}(t) = \bar{B}(t)$. We note that if $\Delta_{\bar{h}} \neq \Delta_{\bar{j}}$, then a quantum critical point can still exist: for instance if $\Delta_{\bar{h}} = \tilde{\alpha}\Delta_{\bar{j}}$, for some constant $\tilde{\alpha}$, then the quantum critical point exists when $\Delta_t = (\tilde{\alpha} - 1)\Delta_{\bar{j}}$, or equivalently $A(t) = B(t) \exp((\tilde{\alpha} - 1)\Delta_{\bar{j}})$.

C. Renormalization-Group Formulation

The analysis that we formulate in this paper for the ARQIM will concentrate on a strong disorder RG approach on the joint distribution functions $p(J(t), l^S(t); \Omega(t))$ and $r(h(t), l^B(t); \Omega(t))$, where $l^B(t)$ is the bond length scale and $l^S(t)$ is the site (spin cluster) length scale. In the RG approach, an energy scale $\Omega(t)$ is introduced [14, 17], defined as the maximum of the bond and coupling strengths, i.e. $\Omega(t) = \max_{ij} (J_{ij}(t), h_i(t))$. The RG analysis proceeds by perturbatively removing the high-energy degrees of freedom, thus reducing the energy scale *at a given instance* in time (hence the distribution functions p and r do not contain an explicit time dependence; instead the time

dependence is followed implicitly as trajectories of the $J(t)$ and $h(t)$ functions). The RG flows will thus provide the appropriate low-energy physical quantities of interest for the given instance in time; after many RG steps the effective distribution functions read $\hat{p}(\hat{J}(t), \hat{l}^S(t); \Omega(t))$ and $\hat{r}(\hat{h}(t), \hat{l}^B(t); \Omega(t))$, with the ‘hat’ notation indicating that renormalization has taken place. The goal is to establish the form of $\hat{p}(\hat{J}(t), \hat{l}^S(t); \Omega(t))$ and $\hat{r}(\hat{h}(t), \hat{l}^B(t); \Omega(t))$.

Specifically, there are two cases to consider when analysing the governing Hamiltonian: $\Omega(t)$ takes either an element from $J(t)$ or an element from $h(t)$. At this stage a rescaling [14, 17] of the random variables is made, through the introduction of the following time-dependent functions

$$\Gamma(t) = \ln \left(\frac{\Omega_I(t)}{\Omega(t)} \right), \quad (8a)$$

$$\zeta(t) = \ln \left(\frac{\Omega(t)}{\hat{J}(t)} \right), \quad (8b)$$

$$\beta(t) = \ln \left(\frac{\Omega(t)}{\hat{h}(t)} \right), \quad (8c)$$

with $\Omega_I(t)$ defined as the initial maximum bond or coupling strength that will stay fixed for a given time instance but that will change with time. After each renormalization step we will, in general, find $\Omega(t) < \Omega_I(t)$, so that $\Gamma(t)$ will become a large parameter in the problem, representing the decrease in the energy scale. Note that $\zeta(t)$ and $\beta(t)$ are strictly non-negative, defined on the interval $[0, \infty)$.

In the case of the problem considered in this work, the rescaled joint distribution functions $\hat{p}(\hat{J}(t), \hat{l}(t); \Omega(t))$ and $\hat{r}(\hat{h}(t), \hat{l}(t); \Omega(t))$ become $\hat{P}(\hat{\zeta}(t), \hat{l}(t); \Gamma(t))$ and $\hat{R}(\hat{\beta}(t), \hat{l}(t); \Gamma(t))$. They satisfy the following integro-differential coupled flow equations (see Appendix for details, and where we have now dropped the ‘hat’ notation for convenience)

$$P_\Gamma - P_\zeta - R_0 P \otimes P - (P_0 - R_0) P = 0, \quad (9a)$$

$$R_\Gamma - R_\beta - P_0 R \otimes R - (R_0 - P_0) R = 0, \quad (9b)$$

and govern the RG flows of the distribution functions for the two independent random variables. Their solution(s) provide the required information about the critical and off-critical flows. It is remarkable that at the critical point, $\delta(t) = 0$, the flow equations uncouple and hence, due to the duality $h_i(t) \longleftrightarrow J_{ij}(t)$, the distribution functions become equivalent. At this point the solution to (9) is straightforward to find as [14]

$$P(\zeta(t), l(t); \Gamma(t)) = a(\Gamma(t)) e^{-a(\Gamma(t))\zeta(t)}, \quad (10a)$$

$$R(\beta(t), l(t); \Gamma(t)) = a(\Gamma(t)) e^{-a(\Gamma(t))\beta(t)}, \quad (10b)$$

where $a(\Gamma(t)) = (\Gamma(t) + 1/a_0)^{-1}$, and where one can show through a suitable stability analysis that this is the critical fixed point. The constant a_0 can be set to zero. We see that this critical flow indicates that the system flows to infinite randomness: the distributions become increasingly broad as $\Gamma(t)$ becomes large (or equivalently $\zeta(t)$ and

$\beta(t)$ small). The duality across the critical point dictates that there exists a duality between the two distribution functions at some time. The remaining analysis will focus on the region near to this critical point, where $\delta(t)$ remains small. In this sense, Δ_t is a measure of the time-dependent ‘distance’ from criticality, that will change as the adiabatic time functions $A_{ij}(t)$ and $B_i(t)$ evolve in time.

III. Transition Through the Quantum Critical Point

Up to now we have concentrated on the ground, or equilibrium, state properties of the time-dependent transverse-field Ising model, using the time as a weighting on the random bond and site couplings. The inclusion of a time in the RG analysis provides the equilibrium critical exponents such as the location of the critical point, magnetisation and correlation length scalings, all parametrised in time. In this section we are interested in the non-equilibrium dynamics that occur as we time-evolve the governing Hamiltonian (Eq. (2)) through the critical point. As we mention earlier, our choice of an adiabatic time evolution is deliberately made in order to remain in the local (in-time) ground state throughout. We thus do not expect any defects - or excited states - to be generated, except in the vicinity of the critical point where the energy gap between the ground state and first excited state will decrease and disappear exactly at the critical point. This is precisely where the computation loses adiabaticity.

It turns out that the analytic scaling for the defect density (a non-equilibrium dynamics) is dependent on knowledge of the equilibrium critical exponents [41, 9]. We will assume for the transition dynamics that we can separate out the time functions from the random variables. Thus we can, by using the equilibrium scalings for the correlation lengths $\xi(t)$, the distance from the critical point $\delta(t)$, and the form of the time functions $A_{ij}(t)$ and $B_i(t)$, find an estimate for the density of defects (or the number of domain walls) that are formed as we transfer through this non-adiabatic region.

To begin, we therefore consider a scaling analysis using the forms of the critical parameter $\delta(t)$ (Eq. (6)), critical correlation length $\xi(t)$, given by

$$\xi(t) = \frac{1}{|\delta(t)|^\nu}, \quad (11)$$

with $\nu = 2$, and the dynamical $z(t)$ exponent, given by

$$z(t) \sim \frac{1}{2|\delta(t)|}, \quad (12)$$

all in the region of the critical point. The energy gap is defined as $\Delta_{\text{gap}} \sim |\delta(t)|^{z(t)\nu} \sim |\delta(t)|^{1/|\delta(t)|}$. We are interested in the region close to the critical point, specifically the region at which the computation loses adiabaticity. This occurs at a critical $\hat{\delta}(t)$ when the energy gap Δ_{gap} is equal to the rate of approach towards the critical point, defined as Δ_{rate} . To find Δ_{rate} we note that we must separately take account of the rate of transition of both of the coupling strengths, $J_{ij}(t)$ and $h_i(t)$. From these, we expect to

be able to write down a characteristic rate $1/\tau$ as

$$\frac{1}{\tau} = \frac{1}{\tau_{\overline{A}(t)}} + \frac{1}{\tau_{\overline{B}(t)}}, \quad (13)$$

where $1/\tau_{\overline{A}(t)}$ and $1/\tau_{\overline{B}(t)}$ represent the characteristic rates of the evolution of the bond and site couplings, respectively. These rates are found through the derivatives of the mean time functions $\overline{A}_{ij}(t)$ and $\overline{B}_i(t)$ evaluated at t_f , the time when the system passes through the critical point. Then $\tau_{\overline{A}(t_f)} = 1/|\dot{A}(t_f)|$ and $\tau_{\overline{B}(t_f)} = 1/|\dot{B}(t_f)|$. For example, if $\overline{A}(t) = (t/T)^2$ and $\overline{B}(t) = 1 - (t/T)^2$ (as in Fig. 2, where we assume $\Delta_{\overline{h}} = \Delta_{\overline{J}}$), then $t_f = T/\sqrt{2}$ and $\tau_{\overline{A}(t_f)} = \tau_{\overline{B}(t_f)} = T/\sqrt{2}$ and $\tau = T/(2\sqrt{2})$. This characteristic rate $1/\tau$ introduces a natural energy scale on the adiabatic evolution of the RG scheme: we can define a critical Γ , defined by $\Gamma_\tau \sim \ln(\Omega\tau)$. We must impose that $\Gamma < \Gamma_\tau$ in order for the RG scheme to be valid in the evolution of the system.

Close to the critical point $\delta(t)$ can be also linearised in time, such that $\delta(t_f) \sim t_f/\tau$, which gives $\Delta_{\text{rate}} = (\tau\delta)^{-1}$. Thus, we can now find $\hat{\delta}$ as the solution to

$$\frac{a}{\tau\hat{\delta}} = \hat{\delta}^{1/|\hat{\delta}|}, \quad (14)$$

where a is a free parameter. We use this result for $\hat{\delta}$, together with the critical correlation length (Eq. (11)), to find that $\hat{\xi} \equiv \xi|_{\hat{\delta}}$ approximates to

$$\hat{\xi} \approx \left(\frac{\log(\tau/a)}{\log[\log(\tau/a)]} - 1 \right)^2 \approx \frac{\log^2(\tau/a)}{\log^2[\log(\tau/a)]}. \quad (15)$$

It is important to note that the choice of functions $A_{ij}(t)$ and $B_i(t)$ enters the above result through the characteristic rate $1/\tau$; in particular we can take $A_{ij}(t)$ and $B_i(t)$ to be nonlinear functions of t/T , as has been considered in the nonrandom transverse-field Ising model [42, 43, 44].

For this adiabatic transition through the critical point, the logarithmic scaling reflects the departure from the typical Kibble-Zurek ($\propto \tau^{1/2}$) scaling that is evidenced in a pure (non-random), or weakly disordered, Ising model. This is the same scaling as found analytically by [9] and numerically by [35], however our analysis, through the inclusion of the time-dependent parameters $A_{ij}(t)$ and $B_i(t)$ into the governing Hamiltonian, has established a generic characteristic timescale that represents a transition through the critical point that is influenced by *both* the bond strengths, $J_{ij}(t)$, and the site strengths, $h_i(t)$.

IV. Discussion and Conclusion

In this work, we have developed and extended the well-established real-space RG approach for quantum chains with randomness [14, 15, 16] to the case of time-dependent Hamiltonians. We took the quantum Ising chain with random terms as an example to

illustrate the protocol of the RG approach. In every step, the parallels and differences from the time-independent case have been noted.

In particular, the location of the quantum critical point, or points, in time depend on the functions that carry the time dependence in the Hamiltonian. This time interval is defined by the time period between the zero of the exchange interaction term in the ARQIM and the zero of the transverse field term. The off-critical flows have been calculated and the ground state properties of the ARQIM have been investigated. In general, the magnetisation as well as the correlation functions retain the form obtained by Fisher [14, 15, 16] and we have indicated in detail where the time enters the calculation.

An important outcome is the connection with the Kibble-Zurek dynamics which govern the system near the critical point. We have constructed a scaling argument for the density of defects as we adiabatically pass through the critical point of the system, in either direction. Our method, thus, provides a justification of the exponents and connects the Kibble-Zurek dynamics with the microscopic time-dependent Hamiltonian.

A further consequence of our calculations is the ability to modify (or shift) the location of the quantum critical point. Such a feature can be of great importance to experiment: one can imagine that a device could be constructed to simulate the quantum critical point. A possible device in this regard would be the development of a long 1D flux qubit chain. Reference [33] has developed a prototype qubit-coupler-qubit device where the governing Hamiltonian is given by Eq. (2) for $N = 2$. In particular the site and bond coupling terms can be assumed to be independent and random, and crucially individually modifiable. In the future we would expect that the length of the qubit chain could be increased to a few thousand qubits. This would put experiment in the N -large limit where the conclusions of this paper could be tested.

The RG approach that we introduce in this paper can be further extended to consider non-integrable spin-chain models, such as the XXZ or next-nearest neighbour Hamiltonians [19, 20, 22, 23] with random interactions. These out-of-equilibrium models admit a many-body localization phase transition that is currently the focus of much interest (see for example [23, 24]). The inclusion of time-dependent functions into these Hamiltonians, along the lines of the adiabatic functions $A(t)$ and $B(t)$ considered in this paper, will allow us to systematically probe (some of the) properties of this transition in further detail. For example, we expect to be able to understand the identified fractal thermal Griffiths regions [24].

The quantity that will enable the characterization of different phases in many different settings is the entanglement entropy. In simpler cases [45], such as out-of-equilibrium steady states of the quantum Ising model, or when perturbations break the integrability, critical boundaries were characterised by the value of the central charge. Following Ref.'s [46, 47], we expect to be able to calculate the distribution of the entanglement entropy for the ARQIM using the real-space RG technique developed in this paper, but in non-integrable spin models, how the time-dependence affects the entanglement entropy especially in connection to many-body localization, is of prime

interest and an open question in this context.

Acknowledgments

We would like to thank Alexander Balanov, Claudio Castellano, John Chalker, Andrey Chubukov, Mike Gunn, Vedika Khemani, David Pekker, Anatoli Polkovnikov and Artur Sowa for insightful discussions that took place during this work. The work was supported by EPSRC through the grant EP/M006581/1.

Appendix

In this appendix we provide further details regarding the renormalization group analysis of Sect. II. We start with Eq. (2), noting that in the first case when the largest coupling is a site, we have $\Omega(t) = h_i(t)$ for some i . The local Hamiltonian for this site and the two adjoining bonds is then $H_{i-1,i+1}^s(t) = -h_i(t)\sigma_i^x - J_{i-1,i}(t)\sigma_{i-1}^z\sigma_i^z - J_{i,i+1}(t)\sigma_i^z\sigma_{i+1}^z$, for adjoining bonds $J_{i-1,i}(t)$ and $J_{i,i+1}(t)$. Under the RG procedure, these adjoining bonds can be treated perturbatively resulting in an effective Hamiltonian for $H_{i-1,i+1}^s(t)$, written as

$$\hat{H}_{i-1,i+1}^s(t) \approx -\hat{J}_{i-1,i+1}(t)\sigma_{i-1}^z\sigma_{i+1}^z, \quad (16a)$$

where

$$\hat{J}_{i-1,i+1}(t) = \frac{J_{i-1,i}(t)J_{i,i+1}(t)}{h_i(t)}. \quad (16b)$$

This is site decimation: a site, $h_i(t)$, and the two adjoining bonds, $J_{i-1,i}(t)$ and $J_{i,i+1}(t)$, are removed and a new bond, $\hat{J}_{i-1,i+1}(t)$ created, joining sites $h_{i-1}(t)$ and $h_{i+1}(t)$. The new bond lengthscale under this decimation becomes $\hat{l}_{i-1,i+1}^B = l_{i-1,i}^B + l_{i,i+1}^B + l_i^S$. As in [14], we set each initial l_i^S and $l_{i,i+1}^B$ equal to $1/2$.

In the second case when the largest coupling is a bond, we have $\Omega(t) = J_{i,i+1}(t)$ for some i . The local Hamiltonian for this bond and two adjoining sites is then $H_{i,i+1}^b(t) = -h_i(t)\sigma_i^x - h_{i+1}(t)\sigma_{i+1}^x - J_{i,i+1}(t)\sigma_i^z\sigma_{i+1}^z$, for adjoining sites $h_i(t)$ and $h_{i+1}(t)$. Under the RG procedure, these adjoining sites can be treated similarly, resulting in an effective Hamiltonian for $H_{i,i+1}^b(t)$, written as

$$\hat{H}_{i,i+1}^b(t) \approx -\hat{h}_i(t)\sigma_i^x, \quad (17a)$$

where

$$\hat{h}_i(t) = \frac{h_i(t)h_{i+1}(t)}{J_{i,i+1}(t)}. \quad (17b)$$

This is bond decimation: a bond, $J_{i,i+1}(t)$, and the two adjoining sites, $h_i(t)$ and $h_{i+1}(t)$, are removed and a new spin cluster, $\hat{h}_i(t)$ created, with adjoining bonds $J_{i-1,i}(t)$ and $J_{i+1,i+2}(t)$. The new spin cluster lengthscale under this decimation becomes $\hat{l}_i^S = l_i^S + l_{i+1}^S + l_{i,i+1}^B$.

The above perturbation analysis formally requires that $\hat{J}_{i-1,i+1}(t)$ is small ($< \epsilon$) for a bond decimation and that $\hat{h}_i(t)$ is small for a site decimation. However, this

stipulation can be somewhat relaxed: errors that result in the initial few steps of the renormalization from invalidity of the perturbation are gradually smoothed away as the number of RG steps increases such that the RG flows become asymptotically valid in the low-energy, long-distance limit.

In the case when we separate out the time functions the criteria for validity of the RG scheme becomes slightly more intricate. To see this, first note that the above expressions for $\hat{J}_{i-1,i+1}(t)$ and $\hat{h}_i(t)$ refer to the distribution functions after a single renormalization step of either bond or site decimation. In general, and after many (bond and site) renormalization steps, a site decimation will give the $\hat{J}_{i-1,i+1}(t)$ as (explicitly separating out the time dependence):

$$\hat{J}_{i-1,i+\hat{l}-1/2}(t) = \frac{\prod_{k=i-1}^{k=i+\hat{l}-3/2} A_{k,k+1}(t) \tilde{J}_{k,k+1}}{\prod_{k=i}^{k=i+\hat{l}-3/2} B_k(t) \tilde{h}_k}, \quad (18a)$$

while a bond decimation will give the $\hat{h}_i(t)$ as

$$\hat{h}_i(t) = \frac{\prod_{k=i}^{k=i+\hat{l}-1/2} B_k(t) \tilde{h}_k}{\prod_{k=i}^{k=i+\hat{l}-3/2} A_{k,k+1}(t) \tilde{J}_{k,k+1}} \quad (18b)$$

where $\hat{l} = n + 1/2$, for integer n , provides the bond or spin cluster length.

While we are able to absorb possible errors during the decimation steps, to end up in the low-energy state, and hence for validity of the RG approach, we must impose that, after many RG steps, a site decimation leads to small $\hat{J}_{i-1,i+\hat{l}-1/2}(t)$ (Eq. (18a)), while a bond decimation satisfies small $\hat{h}_i(t)$ (Eq. (18b)). We must therefore consider the ratio of the time-dependent functions $A_{ij}(t)$ and $B_i(t)$ together with the ratio of the time-independent random distributions. However, these validity arguments must be placed into context with regards to the maximum coupling, as defined in $\Omega(t) = \max_{ij} (J_{ij}(t), h_i(t))$. The functions of time $A_{ij}(t)$ and $B_i(t)$ are fixed during the renormalization process. As such, the cases $A(t) \ll B(t)$ or $A(t) \gg B(t)$ will impose some preference for site or bond decimation, respectively. This indicates that, for $A(t) \ll B(t)$, we would expect a predominance of site decimations while similarly, for $A(t) \gg B(t)$, we would expect a predominance of bond decimations.

In the limit $t \rightarrow T$ (bond strengths dominate; see the expression for $\hat{h}_i(t)$) we expect to recover the form of the distribution functions outlined in [17] for the classical Ising Hamiltonian; there the system presents a self-similar solution where the system flows to infinite randomness as the distribution grows without limit. In this case the distribution functions are given by

$$\hat{p}(\hat{J}(T), \hat{l}(T); \Omega(T)) \rightarrow \frac{1}{\Omega(T)\Gamma(T)} \left(\frac{\Omega(T)}{\hat{J}(T)} \right)^{1-1/\Gamma(T)}, \quad \hat{r}(\hat{h}(T), \hat{l}(T); \Omega(T)) \rightarrow 0, \quad (19)$$

where \hat{l} is the lengthscale that encompasses the history of many site and bond decimations.

Conversely in the special cases when $A_{ij}(t)$ and $B_i(t)$ are time-independent (constant) functions, or when $A_{ij}(t) = B_i(t) \forall i, j$, the results of [14] are recovered: there, a duality is present in the joint distribution functions, and a critical fixed point can be found, again where the system flows to infinite randomness. Then the joint distribution functions at the critical fixed point read (taking the case $A_{ij}(t) = B_i(t)$ that occurs at $t = t_f$) [14, 15]

$$\hat{p}(\hat{J}(t_f), \hat{l}(t_f); \Omega(t_f)) \rightarrow \frac{1}{\hat{\Omega}(t_f)\Gamma(t_f)} \left(\frac{\Omega(t_f)}{\hat{J}(t_f)} \right)^{1-1/\Gamma(t_f)}, \quad (20a)$$

$$\hat{r}(\hat{h}(t_f), \hat{l}(t_f); \Omega(t_f)) \rightarrow \frac{1}{\hat{\Omega}(t_f)\Gamma(t_f)} \left(\frac{\Omega(t_f)}{\hat{h}(t_f)} \right)^{1-1/\Gamma(t_f)}. \quad (20b)$$

We wish to find the form of these distribution functions for all time, along the way recovering the noted special cases. From this point, the ‘hat’ notation will be dropped, and the joint distribution functions will be denoted as $P(\zeta(t), l(t); \Gamma(t))$ and $R(\beta(t), l(t); \Gamma(t))$ with the understanding that they represent the distributions after many renormalization steps, in the limit where $l(t)$ and $\Gamma(t)$ become large.

Given that RG perturbation steps remain valid (Eq’s (18)), we can write down coupled master equations that describe the renormalization flow [14, 17]. To begin, we note that we are interested in those sites $J_{i,i+1}(t)$ or bonds $h_i(t)$ that are in the high energy shell $[\Omega(t) - d\Omega(t), \Omega(t)]$. Equivalently, according to the decimation specifics and the rescalings (Eq.’s (8)) we remove all the sites (bonds) with $0 < \zeta(t) < d\Gamma(t)$ ($0 < \beta(t) < d\Gamma(t)$) and add the appropriate couplings. The additive forms of $\zeta(t)$ and $\beta(t)$, now with the time dependence, still hold; for example we can write that $\zeta_{i-1,i+1}(t) = \zeta_{i-1,i}(t) + \zeta_{i,i+1}(t) + \log(2)$, with the $\log(2)$ enable to be safely neglected in the final reckoning ($\zeta(t) \gg \log(2)$ as $\Gamma(t)$ becomes large). The last consideration is to the effect that time-dependent trajectories, $\zeta(t)$ and $\beta(t)$, have on the flow of the distribution functions. In general therefore, we write $P \rightarrow P + \dot{\zeta} \partial P / \partial \zeta$ and $R \rightarrow R + \dot{\beta} \partial R / \partial \beta$, with the dot representation representing differentiation with respect to time.

Putting all these terms together, and noting that both distribution functions must be normalised, allows us to write down a set of coupled integro-differential flow equations that govern the dynamics of the ARQIM, through the trajectories $\zeta(t)$, $\beta(t)$, $l(t)$ and $\Gamma(t)$, and in terms of the distribution functions $P(\zeta(t), l(t); \Gamma(t))$ and $R(\beta(t), l(t); \Gamma(t))$, as

$$\dot{\zeta} \frac{\partial}{\partial \zeta} [P_\Gamma - P_\zeta - R_0 P \otimes P - (P_0 - R_0) P] = 0, \quad (21a)$$

$$\dot{\beta} \frac{\partial}{\partial \beta} [R_\Gamma - R_\beta - P_0 R \otimes R - (R_0 - P_0) R] = 0, \quad (21b)$$

where subscripts indicate partial differentiation with respect to that variable, and $P_0 = P(\zeta(t) = 0, l(t); \Gamma(t))$ and $R_0 = R(\beta(t) = 0, l(t); \Gamma(t))$. In the above coupled equations, arguments on $P = P(\zeta(t), l(t); \Gamma(t))$ and $R = R(\beta(t), l(t); \Gamma(t))$ have been dropped for brevity.

Integrating up the above equations with respect to $\zeta(t)$ and $\beta(t)$ gives

$$P_{\Gamma} - P_{\zeta} - R_0 P \otimes P - (P_0 - R_0) P = \alpha_1(l(t); \Gamma(t)), \quad (22a)$$

$$R_{\Gamma} - R_{\beta} - P_0 R \otimes R - (R_0 - P_0) R = \alpha_2(l(t); \Gamma(t)), \quad (22b)$$

for ‘constant’ functions $\alpha_1(l(t); \Gamma(t))$ and $\alpha_2(l(t); \Gamma(t))$ independent of $\zeta(t)$ and $\beta(t)$ but possibly dependent on $l(t)$ and $\Gamma(t)$. To find the values of α_1 and α_2 we note that in the special cases when $A_{ij}(t)$ and $B_i(t)$ are time-independent or when $A_{ij}(t) = B_i(t) \forall i, j$, we are in the (non-adiabatic) regime considered by [14], in which case the above equations (22) hold with both α_1 and α_2 equal to zero. This is sufficient information to allow us to safely set $\alpha_1 = \alpha_2 = 0$ always. We are then left with our governing integro-differential coupled flow equations given by Eq.’s (9).

References

- [1] L. E. Sadler, J. M. Higbie, S. R. Leslie, M. Vengalattore, and D. M. Stamper-Kurn, *Spontaneous symmetry breaking in a quenched ferromagnetic spinor Bose-Einstein condensate*, Nature (London) **443**, 312 (2006).
- [2] V. Gritsev, E. Demler, M. Lukin, and A. Polkovnikov, *Spectroscopy of Collective Excitations in Interacting Low-Dimensional Many-Body Systems Using Quench Dynamics*, Phys. Rev. Lett. **99**, 200404 (2007).
- [3] A. Lamacraft, *Quantum Quenches in a Spinor Condensate*, Phys. Rev. Lett. **98**, 160404 (2007).
- [4] A. Läuchli and C. Kollath, *Spreading of correlations and entanglement after a quench in the one-dimensional Bose-Hubbard model*, J. Stat. Mech.: Theor. Exp. **2008**, P05018 (2008).
- [5] A. Flesch, M. Cramer, I. P. McCulloch, U. Schollwöck, and J. Eisert, *Probing local relaxation of cold atoms in optical superlattices*, Phys. Rev. A **78**, 033608 (2008).
- [6] D. Rossini, A. Silva, G. Mussardo, and G. Santoro, *Effective Thermal Dynamics Following a Quantum Quench in a Spin Chain*, Phys. Rev. Lett. **102**, 127204 (2009).
- [7] A. Faribault, P. Calabrese, and J.-S. Caux, *Quantum quenches from integrability: the fermionic pairing model*, J. Stat. Mech.: Theor. Exp. **2009**, P03018 (2009).
- [8] J. Dziarmaga, *Dynamics of a quantum phase transition: Exact solution of the quantum Ising model*, Phys. Rev. Lett. **95**, 245701 (2005).
- [9] J. Dziarmaga, *Dynamics of a quantum phase transition in the random Ising model: Logarithmic dependence of the defect density on the transition rate*, Phys. Rev. B **74**, 064416 (2006).
- [10] A. Polkovnikov, *Universal adiabatic dynamics in the vicinity of a quantum critical point*, Phys. Rev. B **72**, 161201(R) (2005).
- [11] F. Pollmann, S. Mukerjee, A. G. Green, and J. E. Moore, *Dynamics after a sweep through a quantum critical point*, Phys. Rev. E **81**, 020101(R) (2010).
- [12] W. H. Zurek, U. Dorner, and P. Zoller, *Dynamics of a quantum phase transition*, Phys. Rev. Lett. **95**, 105701 (2005).
- [13] J. Eisert, M. Friesdorf, and C. Gogolin, *Quantum many-body systems out of equilibrium*, Nature Physics **11**, 124-130 (2015).
- [14] D. S. Fisher, *Critical behavior of random transverse-field Ising spin chains*, Phys. Rev. B **51**, 6411 (1995).
- [15] D. S. Fisher, *Random transverse field Ising spin chains*, Phys. Rev. Lett. **69**, 534 (1992).
- [16] D. S. Fisher, *Random antiferromagnetic quantum spin chains*, Phys. Rev. B **50**, 3799 (1994).
- [17] G. Refael and E. Altman, *Strong disorder renormalization group primer and the superfluid-insulator transition*, C. R. Physique **14**, 725-739 (2013).
- [18] E. Altman and R. Vosk, *Universal dynamics and renormalization in many-body localized systems*, Annu. Rev. Condens. Matter Phys. **6**, 383-409 (2015).

- [19] R. Vosk and E. Altman, *Dynamical quantum phase transitions in random spin chains*, Phys. Rev. Lett. **112**, 217204 (2014).
- [20] R. Vosk and E. Altman, *Many-body localization in one dimension as a dynamical renormalization group fixed point*, Phys. Rev. Lett. **110**, 067204 (2013).
- [21] A. C. Potter, R. Vasseur, and S. A. Parameswaran, *Universal properties of many-body delocalization transitions*, Phys. Rev. X **5**, 031033 (2015).
- [22] D. Pekker, G. Refael, E. Altman, E. Demler, and V. Oganesyan, *Hilbert-glass transition: new universality of temperature-tuned many-body dynamical quantum criticality*, Phys. Rev. X **4**, 011052 (2014).
- [23] R. Vosk, D. A. Huse, and E. Altman, *Theory of the many-body localization transition in one-dimensional systems*, Phys. Rev. X **5**, 031032 (2015).
- [24] L. Zhang, B. Zhao, T. Devakul, and D. A. Huse, *Many-body localization phase transition: A simplified strong-randomness approximate renormalization group*, Phys. Rev. B **93**, 224201 (2016).
- [25] P. T. Dumitrescu, R. Vasseur, and A. C. Potter, *Scaling Theory of Entanglement at the Many-Body Localization Transition*, Phys. Rev. Lett. **119**, 110604 (2017).
- [26] C. Monthus, *Many-body localization: construction of the emergent local conserved operators via block real-space renormalization*, J. Stat. Mech. **2016**, 033101 (2016).
- [27] C. Monthus, *Periodically driven random quantum spin chains: Real-space renormalization for Floquet localized phases*, arXiv:1702.03165v2.
- [28] A. Lucas, *Ising formulations of many NP problems*, Frontiers in Physics **2**, 2 (2014).
- [29] A. Das and B. K. Chakrabarti, *Colloquium: Quantum annealing and analogue quantum computation*, Rev. Mod. Phys. **80**, 1061 (2008).
- [30] S. Boixo, T. Albash, F. M. Spedalieri, N. Chancellor, and D. A. Lidar, *Experimental signature of programmable quantum annealing*, Nature Comm. **4**, 2067 (2013).
- [31] M. W. Johnson, M. H. S. Amin, S. Gildert, T. Lanting, F. Hamze, N. Dickson, R. Harris, A. J. Berkley, J. Johansson, P. Bunyk, E. M. Chapple, C. Enderud, J. P. Hilton, K. Karimi, E. Ladizinsky, N. Ladizinsky, T. Oh, I. Perminov, C. Rich, M. C. Thom, E. Tolkacheva, C. J. S. Truncik, S. Uchaikin, J. Wang, B. Wilson, and G. Rose, *Quantum annealing with manufactured spins*, Nature **473**, 194-198 (2011).
- [32] Alec Maassen van den Brink, A. J. Berkley, and M. Yalowsky, *Mediated tunable coupling of flux qubits*, New J. Phys. **7**, 230 (2005).
- [33] S. H. W. van der Ploeg, A. Izmailkov, Alec Maassen van den Brink, U. Hübner, M. Grajcar, E. Il'ichev, H.-G. Meyer, and A. M. Zagoskin, *Controllable Coupling of Superconducting Flux Qubits*, Phys. Rev. Lett. **98**, 057004 (2007).
- [34] C. Dasgupta and S.-k. Ma, *Low-temperature properties of the random Heisenberg antiferromagnetic chain*, Phys. Rev. B **22**, 1305 (1980).
- [35] T. Caneva, R. Fazio, and G. E. Santoro, *Adiabatic quantum dynamics of a random Ising chain across its quantum critical point*, Phys. Rev. B **76**, 144427 (2007).
- [36] T. Zanca and G. Santoro, *Quantum annealing speedup over simulated annealing on random Ising chains*, Phys. Rev. B **93**, 224431 (2016).
- [37] M. Kolodrubetz, B. K. Clark, and D. A. Huse, *Nonequilibrium dynamic critical scaling of the quantum Ising chain*, Phys. Rev. Lett. **109**, 015701 (2012).
- [38] F. Iglói, R. Juhász and P. Lajkó, *Griffiths-McCoy Singularities in Random Quantum Spin Chains: Exact Results through Renormalization*, Phys. Rev. Lett. **86**, 1343 (2001).
- [39] F. Iglói, *Exact renormalization of the random transverse-field Ising spin chain in the strongly ordered and strongly disordered Griffiths phases*, Phys. Rev. B **65**, 064416 (2002).
- [40] T. Vojta, *Rare region effects at classical, quantum, and non-equilibrium phase transitions*, J. Phys. A **39**, R143-R205 (2006).
- [41] A. Dutta, G. Aeppli, B. K. Chakrabarti, U. Divakaran, T. F. Rosenbaum and D. Sen, *Quantum Phase Transitions in Transverse Field Spin Models: From Statistical Physics to Quantum*

- Information*, (Cambridge University Press, Cambridge, 2015).
- [42] R. Barankov and A. Polkovnikov, *Optimal Nonlinear Passage Through a Quantum Critical Point*, Phys. Rev. Lett. **101**, 076801 (2008).
 - [43] S. Mondal, K. Sengupta, and D. Sen, *Theory of defect production in nonlinear quench across a quantum critical point*, Phys. Rev. B **79**, 045128 (2009).
 - [44] D. Sen, K. Sengupta, and S. Mondal, *Defect Production in Nonlinear Quench across a Quantum Critical Point*, Phys. Rev. Lett. **101**, 016806 (2008).
 - [45] R. Cole, F. Pollmann and J. J. Betouras, *Entanglement scaling and spatial correlations of the transverse field Ising model with perturbations*, Phys. Rev. B **95**, 214410 (2017).
 - [46] G. Refael and J. E. Moore, *Entanglement Entropy of Random Quantum Critical Points in One Dimension*, Phys. Rev. Lett. **93**, 260602 (2004).
 - [47] T. Devakul, S. N. Majumdar, and D. A. Huse, *Probability distribution of the entanglement across a cut at an infinite-randomness fixed point*, Phys. Rev. B **95**, 104204 (2017).